Journal of Magnetics 16(1), 36-41 (2011) DOI: 10.4283/JMAG.2011.16.1.036

Feasibility Study on the Utilization of EMAT Technology for In-line Inspection of Gas Pipeline

Sung-Ho Cho[1,2]*, Hui-Ryong Yoo[1], Yong-Woo Rho[1], Hak-Joon Kim[2], Dae-Kwang Kim[2], Sung-Jin Song[2], and Gwan Soo Park[3]

[1]R&D Division, Korea Gas Corporation, Incheon 406-130, Korea
[2]School of Mechanical Engineering, Sungkyunkwan University, Suwon 440-746, Korea
[3]School of Electrical Engineering, Busan National University, Busan 609-735, Korea

(Received 25 August 2010, Received in final form 24 November 2010, Accepted 24 November 2010)

If gas is leaking out of gas pipelines, it could cause a huge explosion. Accordingly, it is important to ensure the integrity of gas pipelines. Traditionally, over the years, gas-operating companies have used the ILI system, which is based on axial magnetic flux leakage (MFL), to inspect the gas pipelines. Relatively, there is a low probability of detection (POD) for the axial defects with the axial MFL-based ILI. To prevent the buried pipeline from corrosion, it requires a protective coating. In addition to the potential damage to the coating by environmental factors and external forces, there could be defects on the damaged coating area. Thus, it is essential that nondestructive evaluation methods for detecting axial defects (axial cracks, axial groove) and damaged coating be developed. In this study, an electromagnetic acoustic transducer (EMAT) sensor was designed and fabricated for detecting axial defects and coating disbondment. In order to validate the performances of the developed EMAT sensor, experiments were performed with specimens from axial cracks, axial grooves, and coating disbondment. The experimental results showed that the developed EMAT sensor could detect not only the axial cracks (minimum 5% depth of wall thickness) and axial grooves (minimum 10% depth of wall thickness), but also the coating disbondment.

Keywords : axial defects, coating disbondment, EMAT, gas pipes, NDE

1. Introduction

In-line inspection (ILI) systems based on various nondestructive evaluation methods have been developed and applied for inspecting defects in gas pipelines in some developed countries.

Generally, magnetic flux leakage (MFL) and ultrasonic tools have been used widely for inspecting pipelines. Nevertheless, gas operation companies have mostly chosen MFL tools because ultrasonic tools require couplants for inspection of the gas pipeline. For protection of the buried gas pipeline from corrosion, cathodic protection (CP) provides the necessary protective coating. Because the coating could be damaged by environmental factors and external forces, there also could be many defects upon this damaged coating area, like metal loss of wall thickness. Normally, a direct current voltage gradient (DCVG) or close interval potential survey (CIPS) method has been used to detect the damaged coating. However, these methods require extensive time for inspection and there are many non-inspected areas like asphalt roads. Therefore, it is very important for the gas operators to detect the damaged coating, as well as defects, because the damaged coating finally results in various defects due to the very excessive inflow or outflow of the cathodic current. Until recently, detection of corrosion defects and damaged coatings have been kept separate. Thus, gas operators have focused upon utilizing electromagnetic acoustic transducer (EMAT) technology for ILI of gas pipeline until now because the EMAT technology can detect axial defects that have low probability of detection (POD) in an inspection that simultaneously employs an axial MFL tool and damaged coating. In order to apply EMAT technology for ILI of gas pipeline, it is essential that the EMAT sensor, consisting of coils and magnets, be designed and fabricated. Such an EMAT sensor should be designed by considering the following: shape of the coil; dimension of the coil;

*Corresponding author: Tel: +82-32-810-0343
Fax: +82-32-810-0339, e-mail: shcho@kogas.or.kr

space between the coils.

Therefore, in this study, the EMAT sensor was designed and fabricated to detect axial defects and coating disbondment. Moreover, the experiments were performed with specimens containing axial cracks, axial grooves, and coating disbondment in order to validate the performance of the developed EMAT sensor.

2. Principle of the SH EMAT Technology for Detecting Axial Defect and Coating Disbondment

A generated shear horizontal (SH) guided wave propagates from the EMAT sender towards the EMAT receiver, along the pipe wall and the coated area in the circumferential direction as shown in Fig. 1(a). Under zero-defect conditions, this SH guided wave reaches the receiver and is recorded as a transmission signal. If there are defects like cracks between the EMAT sender and the EMAT receiver, part of the SH guided wave is reflected in the direction of the EMAT sender. In addition, the transmission signal amplitude decreases as shown in Fig. 1(c). While an SH guided wave propagates through the pipe wall, the wave leaks into the coating, which can dampen the wave.

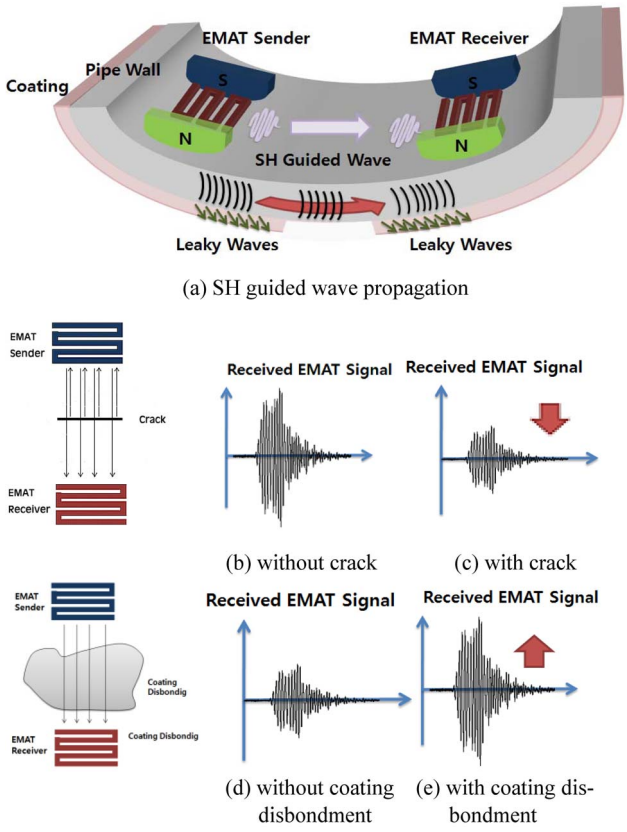

Fig. 1. Principle of detecting axial defects (crack) and coating disbondment using EMAT.

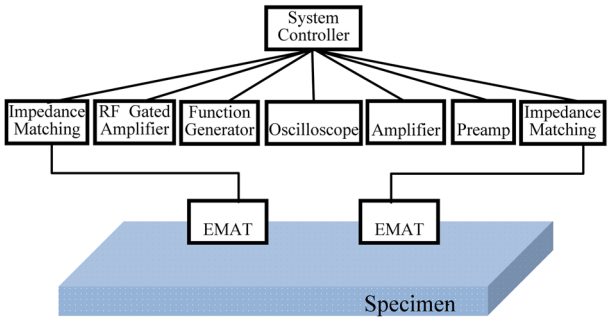

Fig. 2. Schematic diagram of an EMAT system.

Hence, if the damping disappears, there would be a significant increase in the transmission signal amplitude, as shown in Fig. 1(e) [1, 2].

3. Design and Fabrication of the SH EMAT Sensor

3.1. EMAT system

As shown in Fig. 2, the EMAT system consists of a function generator to generate the tone-burst sine wave, system controllers to control a function generator, an RF gated amplifier to amplify the generated wave, an amplifier to amplify the received signal, a digital oscilloscope to save the signals, impedance matching network to improve the efficiency of sending and receiving, and finally EMAT sensors to generate and receive the guided wave. In this study, for a good impedance matching, EMAT sensors were coupled to the RF gated amplifier and preamplifier through an LC impedance matching network [3].

3.2. Design of SH EMAT sensor

An EMAT sensor was designed and fabricated for inspecting a gas pipe specimen with artificial axial defects and coating disbondment. Normally, there are two basic types of EMAT sensor structures [4]. One is a Lorentz force EMAT using a meander coil, and the other is a magnetostrictive force EMAT that employs a meander

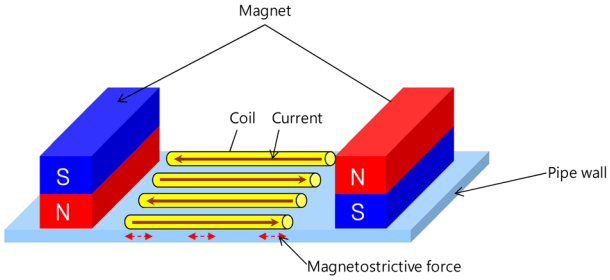

Fig. 3. Structure of a magnetostrictive force EMAT using a meander coil.

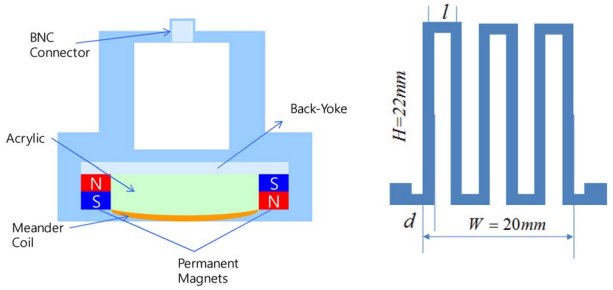

(a) (b)

Fig. 4. Schematic diagrams of (a) the designed EMAT sensor and (b) the designed meander coil.

coil. In this study, the structure of a magnetostrictive force EMAT, using bias magnets to apply magnetic field to magnetic conductor and meander coil to interact with a static magnetic bias (Fig. 3), was chosen as the latter is more robust than the former, while the latter is more effective when considering ILI system.

In order to fabricate an EMAT sensor for generating an SH guided wave, an EMAT sensor capable of generating a non-dispersive SH0 mode, having a constant velocity regardless of generating frequency, was designed. Schematic diagrams of the designed EMAT sensor and the designed meander coil are shown in Fig. 4.

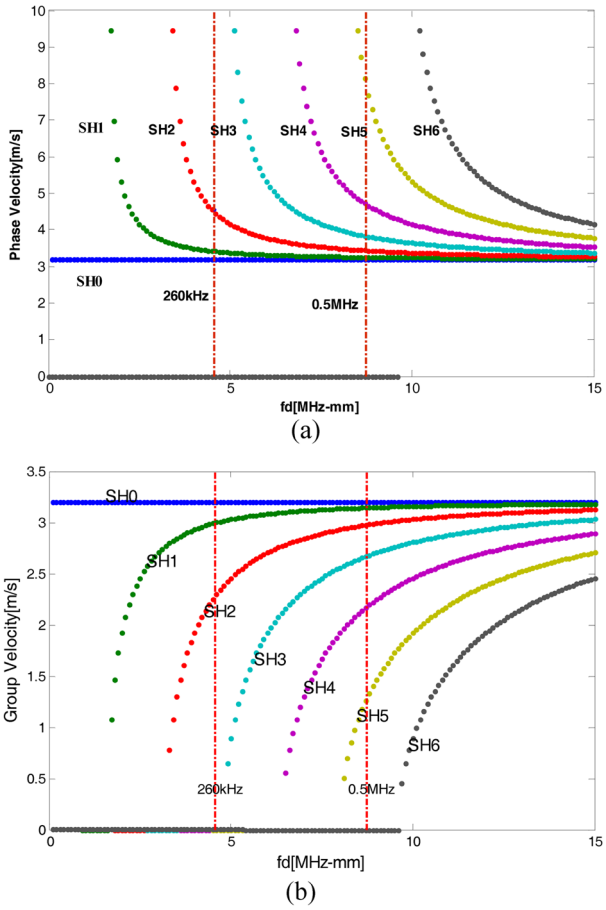

Fig. 5. The (a) phase velocity (b) group velocity dispersion curves of the SH wave for a gas pipe specimen.

Fig. 5 shows phase velocity dispersion and group velocity dispersion curves of SH waves on a gas pipe specimen. As shown in Fig. 5, the SH0 mode can be generated throughout all frequencies. As the generating frequency becomes higher, many dispersive modes are developed in addition to the SH0 mode [5]. Therefore, a low center frequency is better than a high to avoid the dispersive modes. But at a low frequency, energy consumption of the ILI system is higher than at the high frequency. Also, the POD of the coating disbondment is more effective at the high frequency. Therefore, the center frequency should be determined by considering dispersive modes, energy consumption, and material to inspect. In this study, since the high-pass filter of the EMAT receiver system used is not adjustable below 0.26 MHz, the EMAT sensor with a center frequency below 0.26 MHz cannot be applied. Over 0.26 MHz, at a center frequency of 0.5 MHz, the most effective signals could be acquired through the experiment. Therefore, the meander coil with a center frequency of 0.5MH is applied towards the EMAT sensor.

To improve the efficiency of sending and receiving of the guided wave, an EMAT sensor with a two-layered meander coil was designed. A permanent magnet was used (Nd-Fe-B; 8 mm length, 4 mm width, 25 mm height). Design parameters d and l in Fig. 4(b) were determined by Eq. (1) and (2). A meander coil was made inflexible plate by a printing method.

The acquired shear wave velocity was 3,202 m/s. A reflection signal from the bottom surface of a gas pipe specimen, by a pulse-echo method with shear piezoelectric transducer, was used to measure the shear wave velocity:

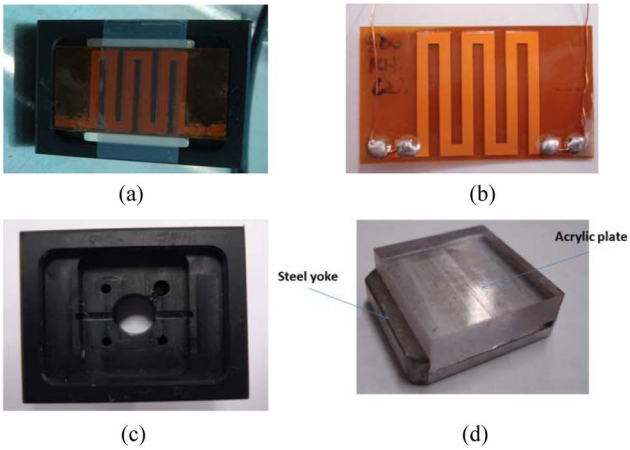

(a) (b) (c) (d)

Fig. 6. Photos of the fabricated SH-EMAT sensor: (a) SH-EMAT sensor; (b) meander coil; (c) case; (d) steel yoke and acrylic plate.

$$l = \frac{C_s}{2f} = \frac{3.202\ \text{mm/}\mu\text{s}}{2 \times 0.5\ \text{MHz}} = 3.2\ \text{mm} \quad (1)$$

$$d = \frac{l}{2} = 1.6\ mm \quad (2)$$

where l is the interval between meander coils, d the width of the meander coil, C_s the shear wave velocity, and f the center frequency. Fig. 6 shows the fabricated SH EMAT sensor and the components of the sensor.

4. Experiments

Experiments were performed to verify performance of the developed SH EMAT sensor. Three specimens with artificial defects were fabricated. The first specimen had axial cracks with depths of 5, 10, 30, 50, 70, and 90% of the wall thickness (17.5 mm), 50 mm length, and 0.2 mm width. The second specimen had axial grooves with depths of 10, 20, 30, and 50% of the wall thickness (17.5 mm), 35 mm length, and 17.5 mm width. The third specimen had coating disbondment, 50 mm length and 100 mm width. Fig. 7 shows photos of the fabricated gas pipe specimens with defects.

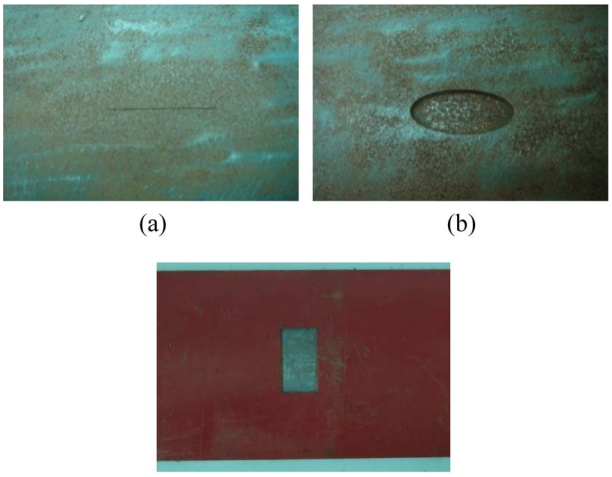

Fig. 7. Photos of the fabricated gas pipe specimens with: (a) axial crack (depth: 30%); (b) axial groove (depth: 30%); (c) a coating disbondment.

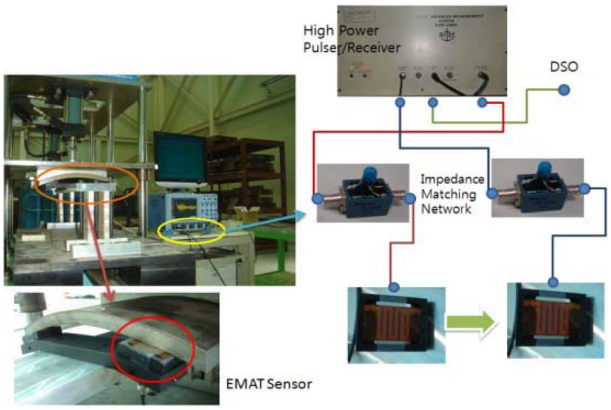

Fig. 8. Experimental setup for evaluating the developed EMAT sensor.

As shown in Fig. 8, an EMAT system was built to evaluate the performance of the developed SH-EMAT sensor. As mentioned before, EMAT system consists of a high-power pulser/receiver to generate a tone-burst signal, a control PC, an impedance matching network, SH-EMAT sensors with a center frequency of 0.5 MHz, and a DSO (digital storage oscilloscope).

5. Evaluation Results

As shown in Fig. 9, defects are located between an EMAT sender and an EMAT receiver. Transmission signals were investigated with respect to defects.

Fig. 10 (a) Comparison of acquired transmission signal

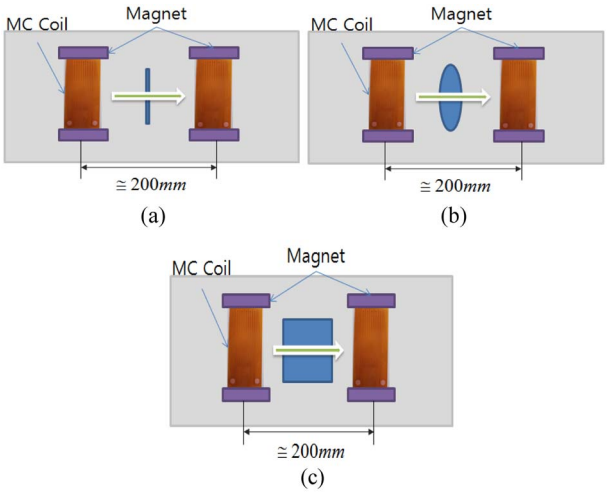

Fig. 9. Schematic diagrams of the position of: (a) an axial crack; (b) an axial groove; (c) a coating disbondment (MC: Meander Coil).

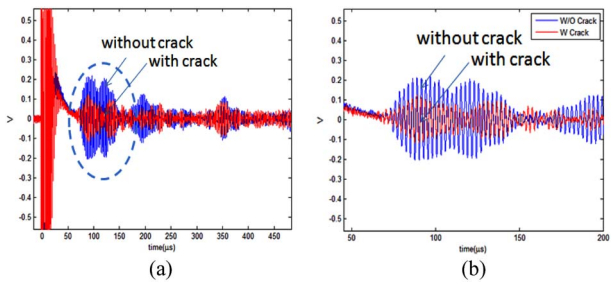

Fig. 10. (a) Comparison of acquired transmission signal without axial cracks to one with an axial crack and (b) zoom-in windowed signal of the circular portion in Fig. 10(a).

without axial cracks to one with an axial crack and (b) zoom-in windowed signal of the circular portion in Fig. 10(a).

5.1. Detection of axial cracks

Fig. 10 shows a comparison of the transmission signal without an axial crack to one with an axial crack, at a depth of 10% of the wall thickness (17.5 mm). As shown in Fig. 10, the transmission signal amplitude decreases in the case of the specimen with axial cracks. As the depth of defects becomes deeper, the amplitude of the transmission signal decreases as shown in Fig. 11.

5.2. Detection of axial grooves

Figure 12 shows comparison of transmission signals without axial grooves to those with axial grooves with depths 50% of the wall thickness (17.5 mm). As shown in Fig. 12, the transmission signal amplitude decreases in the case of specimens with an axial groove. As the depth of the defects becomes deeper, the energy of the transmission signal decreases as shown in Fig. 13.

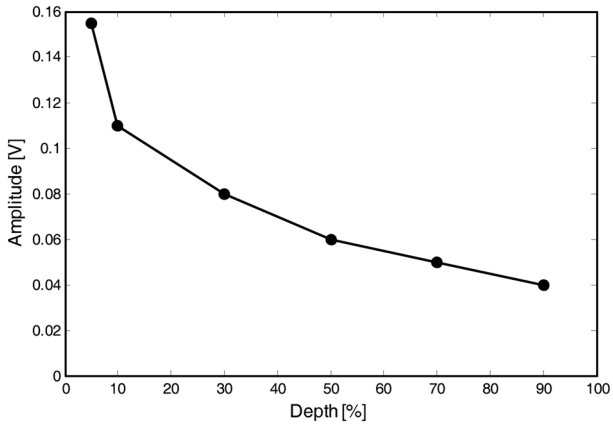

Fig. 11. Measured transmission signal with cracks of varying depth.

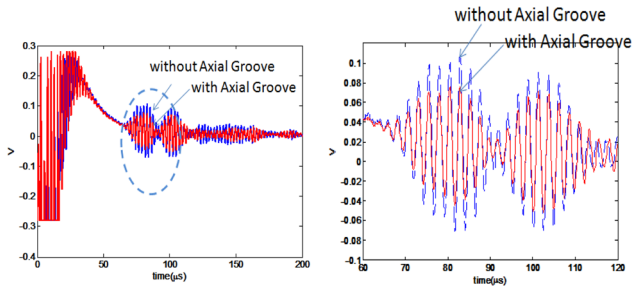

(a) (b)

Fig. 12. (a) Comparison of acquired transmission signals without an axial groove to those with an axial groove and (b) zoom-in windowed signals of the circular portion of Fig. 12(a).

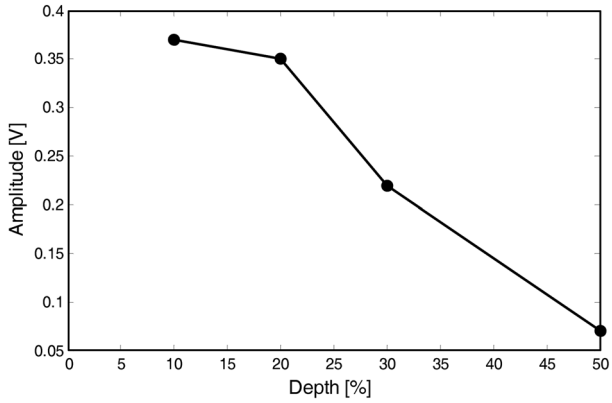

Fig. 13. Measured transmission signal with grooves of varying depth.

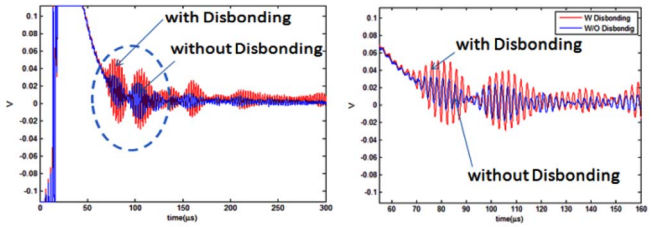

(a) (b)

Fig. 14. (a) Comparison of acquired transmission signals without coating disbondment to those with coating disbondment and (b) zoom-in windowed signal of the circular portion of Fig. 14(a).

5.3. Detection of coating disbondment

Fig. 14 shows comparison of transmission signals without coating disbondment to those with coating disbondment. As shown in Fig. 14, the transmission signal amplitude increases in the case of the specimen with a coating disbondment.

6. Summary

In this study, EMAT sensors were designed and fabricated to detect axial defects and coating disbondment in a gas pipeline. Major design parameters were determined on the dispersion characteristics of the guided waves in the gas pipeline. Using the determined parameters, EMAT sensors that could generate and receive the SH wave were fabricated. Moreover, experiments were performed with specimens in axial cracks, axial grooves, and coating disbondment to validate performance of the developed EMAT sensor. The EMAT sensor developed in this study could detect not only axial groove (depth of 10% of wall thickness) and axial cracks (depth of 5% of wall thickness), but also coating disbondment.

References

[1] J. Aron, J. Gore et al., Development of an EMAT In-Line Inspection System for Detection, Discrimination, and Grading of Stress Corrosion Cracking in Pipelines, Annual Technical Progress Report, Tuboscope Pipeline Services (2001) pp. 11-12.

[2] Thomas Beuker and Joerg Damaschke, In-line Inspection with High Resolution EMAT Technology Crack Detection and Coating Disbondment, Rosen Technology & Research Center, 20th international Pipeline Pigging, Integrity Assessment & Repair Conference (2008).

[3] M. Hirao and H. Ogi, EMATs for Science and Industry - Nondestructive Ultrasonic Measurements, Kluwer Academic Publishers, Boston (2003) pp. 73-75.

[4] R. B. Thompson, Measurements with EMAT Transducer, Physical Acoustics Vol.XIX, Academic Press, Burlington, MA (1990) pp. 192-196.

[5] J. L. Rose, Ultrasonic Waves in Solid Media, Cambridge University Press, Cambridge (2000) pp. 101-113.